

SUPPLEMENTARY FIGURE LEGENDS

Figure S1. Phenotype screening of tagged and deletion strains. Spotting assays comparing the growth of the various tagged, deletion, and wild-type strains used in this study. The cells were grown in culture to log phase, then adjusted to equal concentrations and diluted by 1:10 for each dilution. Spotting assays were performed on either YPD plates or on YPD plates containing 200 mM hydroxyurea.

Figure S2. Regions used to identify H2A.Z incorporation values for -1 and +1 nucleosomes. Heat map showing the regions over which the +1 nucleosome, NDR, and -1 nucleosomes predominantly fall. Within these windows a +1 nucleosome, NDR, and -1 nucleosome value was called for each gene. For +1 nucleosomes this value corresponds to the maximum signal within 15 consecutive 10 bp bins (for 150 bp) between -50 and 150 bp surrounding the annotated TSS. For -1 nucleosomes this value corresponds to the maximum signal within 15 consecutive 10 bp bins between -350 and -100. For NDRs the value corresponds to the minimum signal within 5 consecutive 10 bp bins (for 50 bp) between -200 to 0.

Figure S3. H2A.Z MNase ChIP-seq replicates and averaged data. Heatmap representations of input normalized H2A.Z occupancy around 5797 annotated gene TSS. The two replicates showed very similar occupancy patterns, so the average of the two replicates (right panel) was taken and was used for further analyses.

Figure S4. Swr1 binds its own promoter. The region shown corresponds to the close-up shown in Fig. 2A, but the background has been equalized between tracks. The ChIP-seq signal in the *htz1Δ* mutant is greatly reduced (seen from the increased background compared to signal in this track), compared to the wildtype strain. The 4th row contains H2A.Z ChIP-seq data, and the last row input data for comparison. Here, the y-axis has been scaled so as to optimally show the peak in the 4th track.

Figure S5. H2A.Z does not affect expression of Swr1 or Ino80. Immunoblots showing expression of Myc-tagged Swr1 and Ino80 used for ChIP. Protein extracts

were transferred to PVDF membranes which were then cut into top and bottom halves based on molecular weight markers. The top was probed with an anti-Myc antibody and the bottom was probed with an anti-Actin antibody. Images were assembled by cropping the correctly sized bands for each protein or the corresponding region of the blot for the negative control.

Figure S6. H2A.Z occupancy at the +1 nucleosome compared to Swr1 binding. (A) Input-normalized H2A.Z +1 nucleosome occupancy levels plotted against the Swr1 signal around the NDR (-350 to 150) with outliers dropped. (B) The same H2A.Z data as in A, sorted by the Swr1 signal rank and including outliers. (C) Input-normalized +1 H2A.Z occupancy data plotted against the Swr1 signal within the NDR (-200 to 0). (D) Gene expression levels (read count normalized by transcript length) plotted against the Swr1 signal around the NDR (-350 to 150). (E) Correlation of signal strength at promoter regions between H2A.Z occupancy in our data and published Swr1 occupancy measured using ChIP-exo (50). (F) Genome-wide rank correlation between ChIP-seq signal in 100 bp bins comparing our data to published Swr1 binding data (ref 49 = Henikoff 2015, ref 50 = Pugh 2018). Rep indicates biological replicate. The Spearman correlation coefficient was calculated using Galaxy (usegalaxy.org).

Figure S7. Swr1 occupancy separated by gene orientation. (A) Violin plots of Swr1 occupancy across the NDR (-350 to 150) of all annotated gene TSS separated by the gene orientation around the TSS. The average occupancy does not vary significantly based on gene orientation. Values are normalized against input samples. (B) H2A.Z occupancy levels at gene groups determined based on the intensity of input-corrected Swr1 binding at the NDR, as measured by the total signal between -350 to +150. This window was picked to encompass all NDR-associated binding, whether at the -1 nucleosome, NDR, or +1 nucleosome (see Fig. S2 for region estimates). In the plots, the dark line represents the average normalized signal, and the lighter shaded envelope represents the 95% confidence interval. Altogether, 2598 genes were classified as having a tandem orientation and 3190 as divergent.

Figure S8. Correlation between Swr1 and Ino80 occupancy. Normalized Swr1 and Ino80 ChIP-seq occupancy signals around the NDR are plotted.

Figure S9. Correlation of H2A.Z occupancy with gene expression and RNA Pol II Ser-5P levels. (A) This figure displays the same H2A.Z occupancy data as in Fig. 4B, plotted instead against the log transformed gene expression level measured as read counts, normalized by gene length. (B) Heat map displaying H2A.Z incorporation across gene TSS regions when sorted by RNA Pol II Ser-5P levels (measured by read counts from ChIP-seq of RNA Pol II Ser-5P). The H2A.Z occupancy data on the right is sorted according to the Pol II Ser-5P occupancy data on the left.

Figure S10. Expression of upstream antisense noncoding (UAN) RNAs. RNA-seq data from SMORE-seq (this study) or NET-seq (44) is plotted to show the expression of UAN RNAs upstream of TSS. Only ORFs in the tandem arrangement were chosen and RNA-seq reads mapping to the opposite strand are plotted in the heatmap to display antisense transcription.

Figure S11. The same analysis as in Figure 5A, except that UAN RNAs from NET-seq analysis were used to rank the H2A.Z occupancy profiles.

Figure S12. Average profiles of H2A.Z occupancy separated by TSS orientation. (A) H2A.Z MNase ChIP-seq profiles show that H2A.Z incorporation into the -1 nucleosome differs dramatically between divergent and tandem transcripts. By contrast, the input MNase seq profiles show little difference between the two groups. (B) Same data as in A, but after input-normalization of H2A.Z MNase-ChIP to standard MNase background nucleosomes.

Figure S13. Transcriptional characteristics of TATA-box containing genes. Box plots showing gene expression levels and upstream antisense transcription (UAN-RNAs) from TATA-box containing and TATA-less genes where the upstream gene is in tandem orientation. *p*-values were calculated by Welch's t-test.

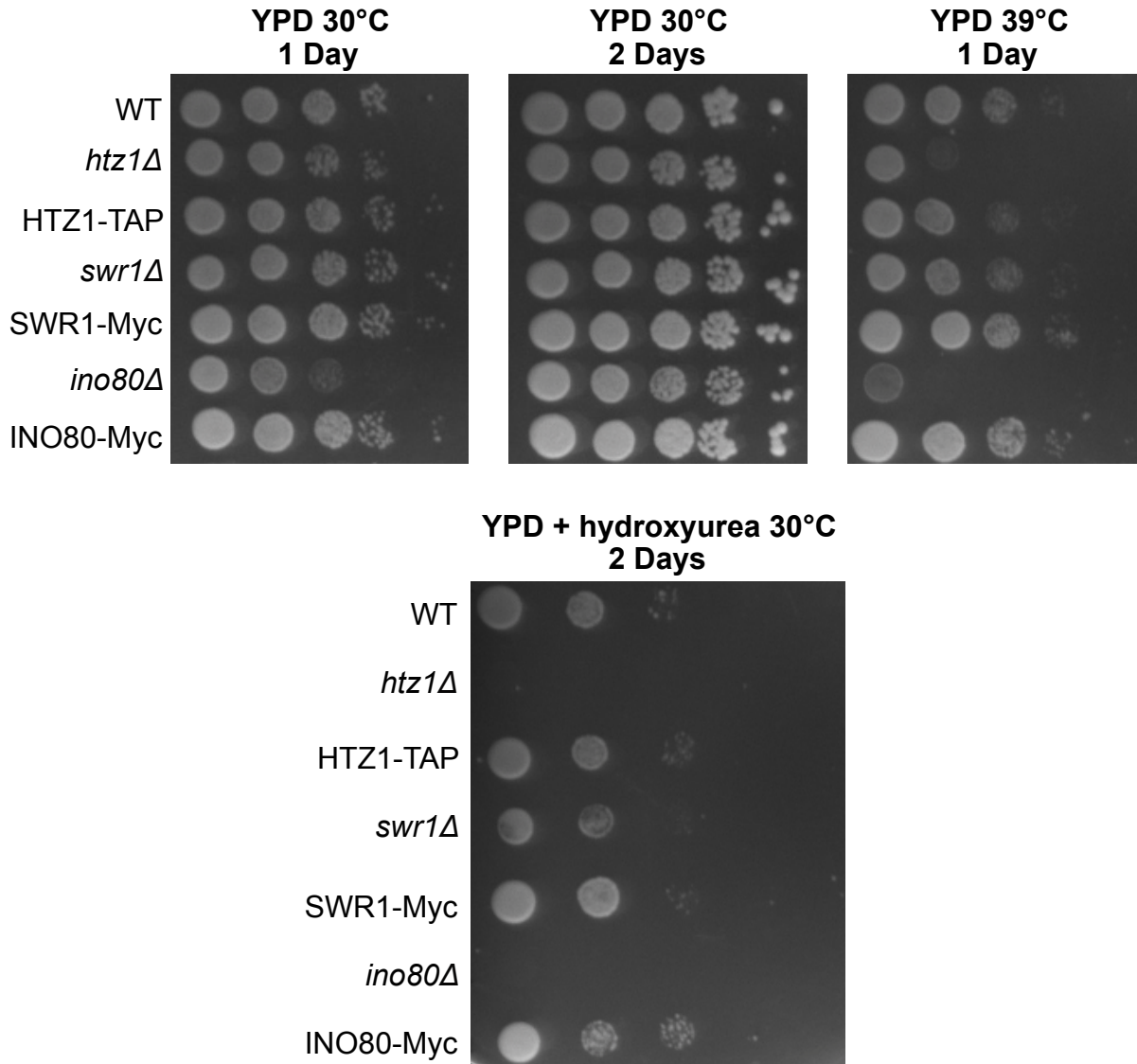
Figure S14. Boxplots of H2A.Z incorporation at +1 nucleosomes of TATA box-containing and TATA-less promoters. H2A.Z occupancy at the +1 nucleosome, separated by the presence or absence of a TATA box. Genes with TATA boxes display significantly less incorporation of H2A.Z, whether they are tandem or divergent.

Figure S15. Swr1 and Ino80 localization at highly expressed genes in *htz1Δ*. (A) Average binding profiles of Swr1 across the TSS for the 500 most highly expressed genes and for all genes. (B) Average binding profiles of Ino80 across the TSS for the 500 most highly expressed genes and for all genes.

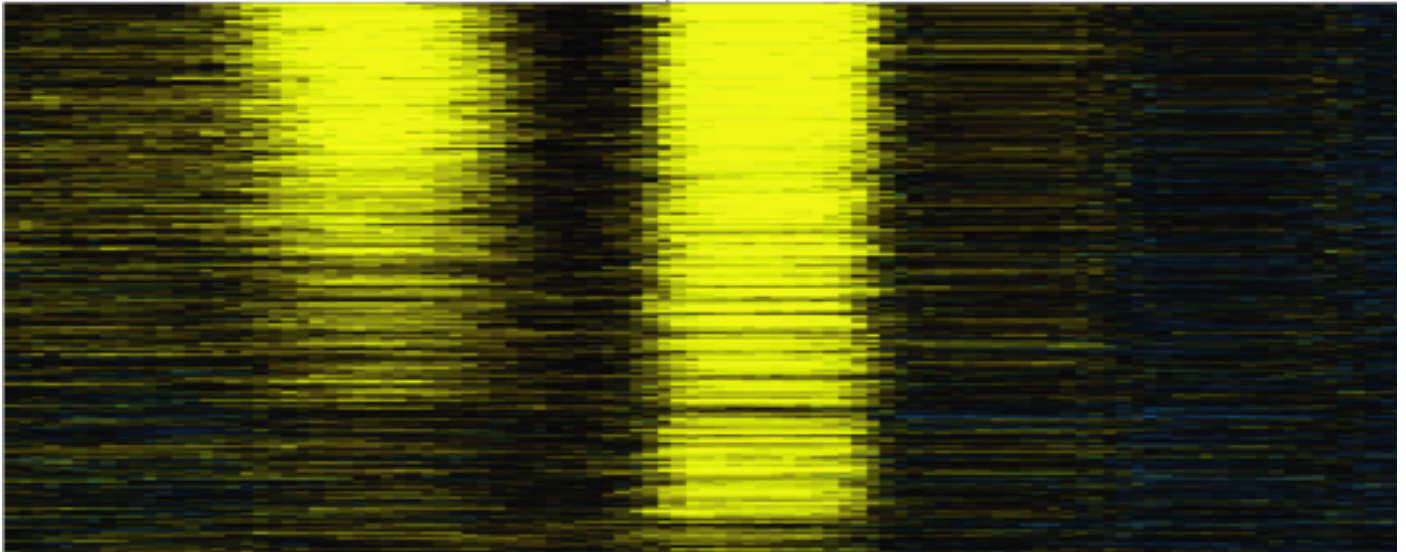
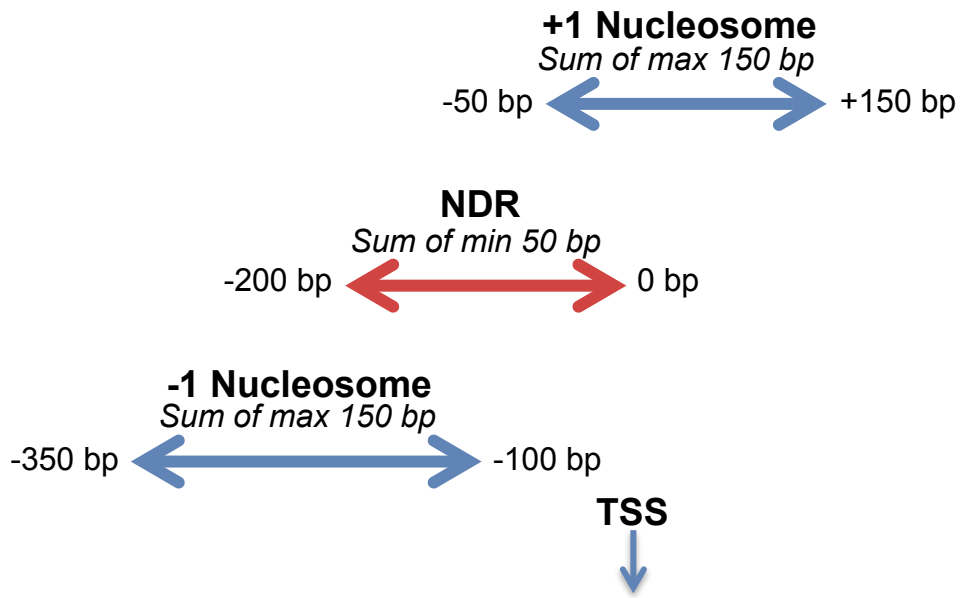
Figure S16. H2A.Z occupancy at TATA-containing promoters after Ino80 depletion. Occupancy data is from Tramantano et al (9) where H2A.Z occupancy was measured after conditional depletion of Ino80. TATA-less, RP genes and TATA-containing genes are arranged as indicated on the left. Although there is lower H2A.Z occupancy at TATA-containing genes (see Fig. 7A, B), there is no difference in this behavior when Ino80 is depleted.

Figure S17. H2A.Z incorporation and directionality in relation to intron status. (A) Average H2A.Z occupancy at the NDR and surrounding regions in the different classes of genes as indicated. 115 RP genes contain introns. (B) Boxplot of antisense transcription levels showing differences between the three classes of genes. *p*-values were calculated by Welch's t-test. NS = not significant. Values represent counts of reads mapping between -50 bp and -300 bp upstream of the TSS on the antisense strand. (C) Boxplot of sense transcription levels (gene expression) between the three classes of genes. *p*-values were calculated by Welch's t-test. Values represent counts of reads mapping to each transcript, normalized by gene length.

Supplementary Figure S1

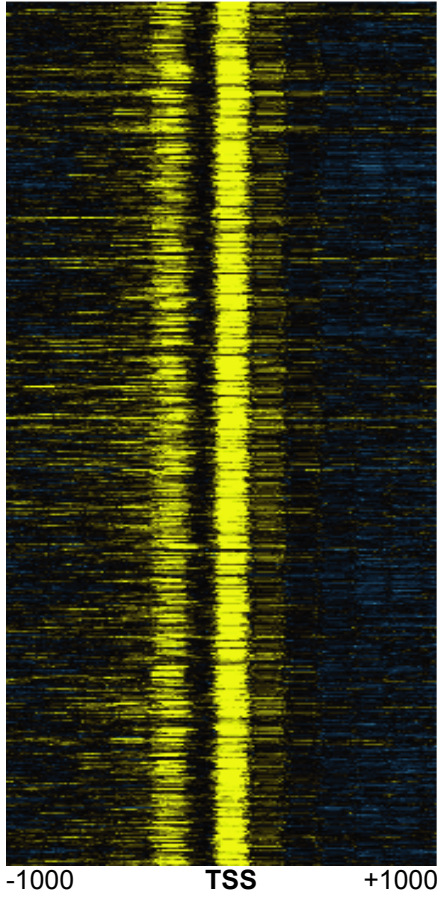


Supplementary Figure S2

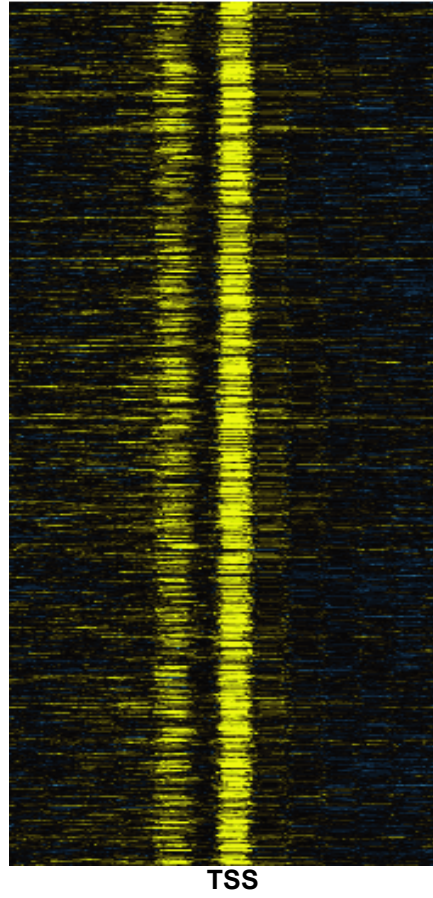


Supplementary Figure S3

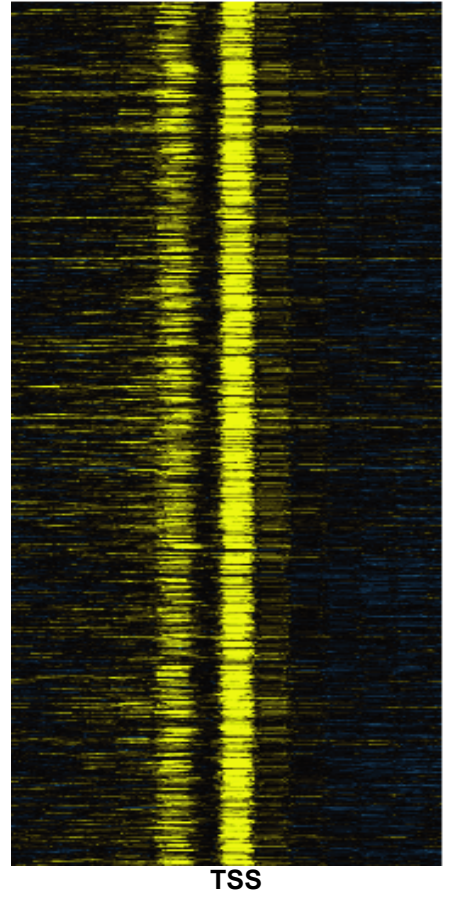
Replicate 1



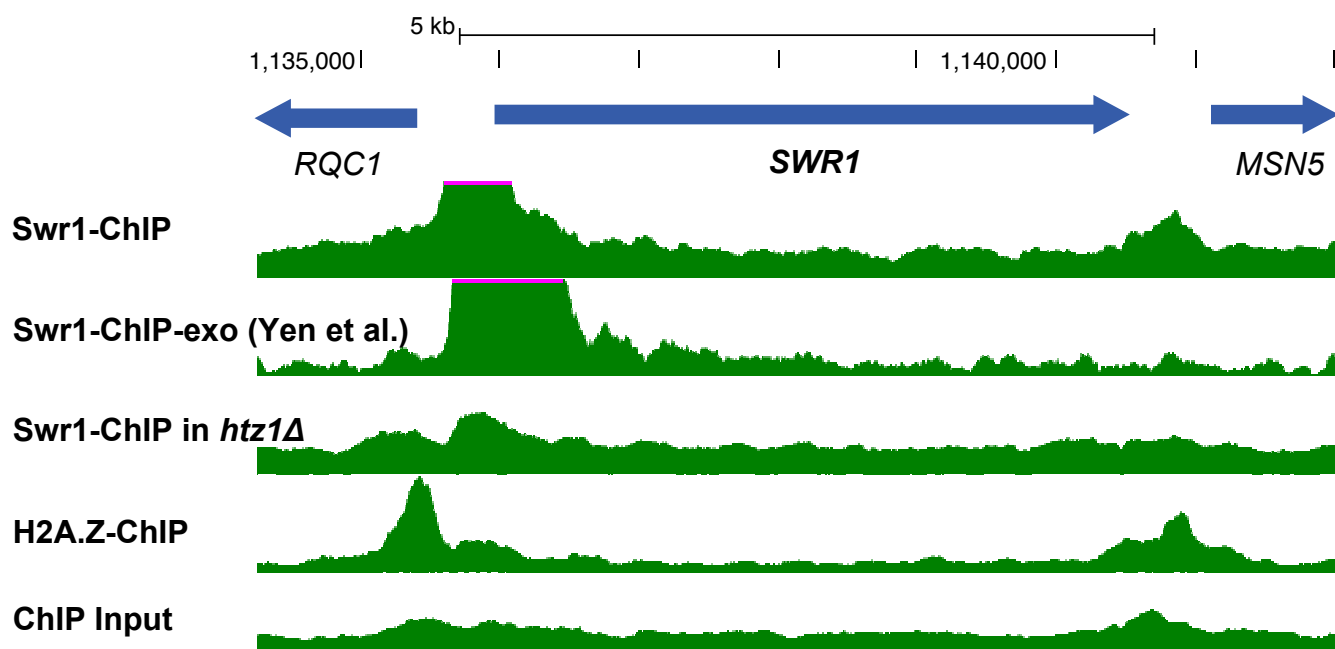
Replicate 2



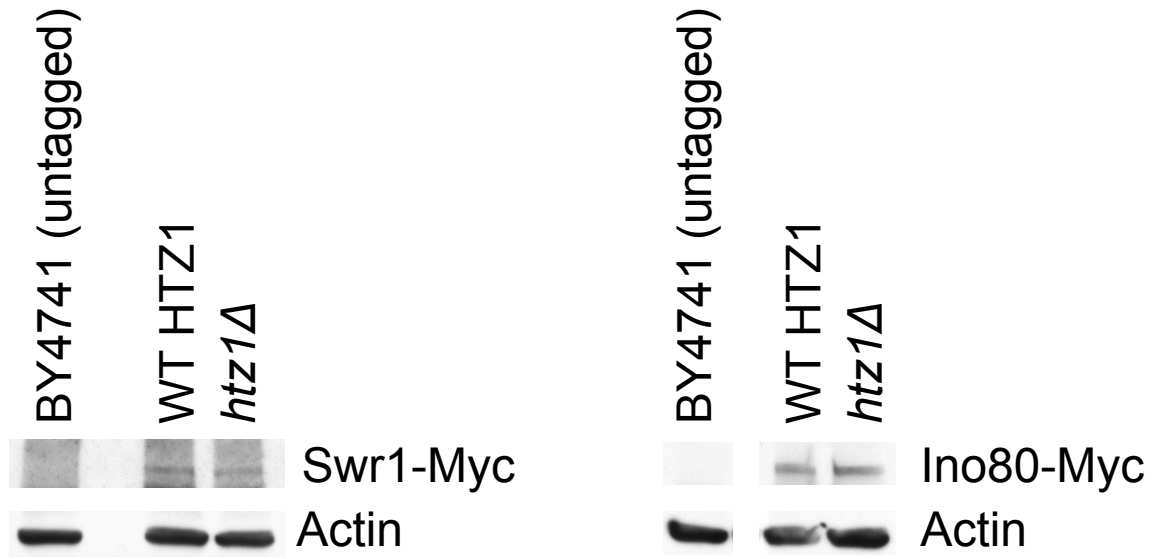
Average



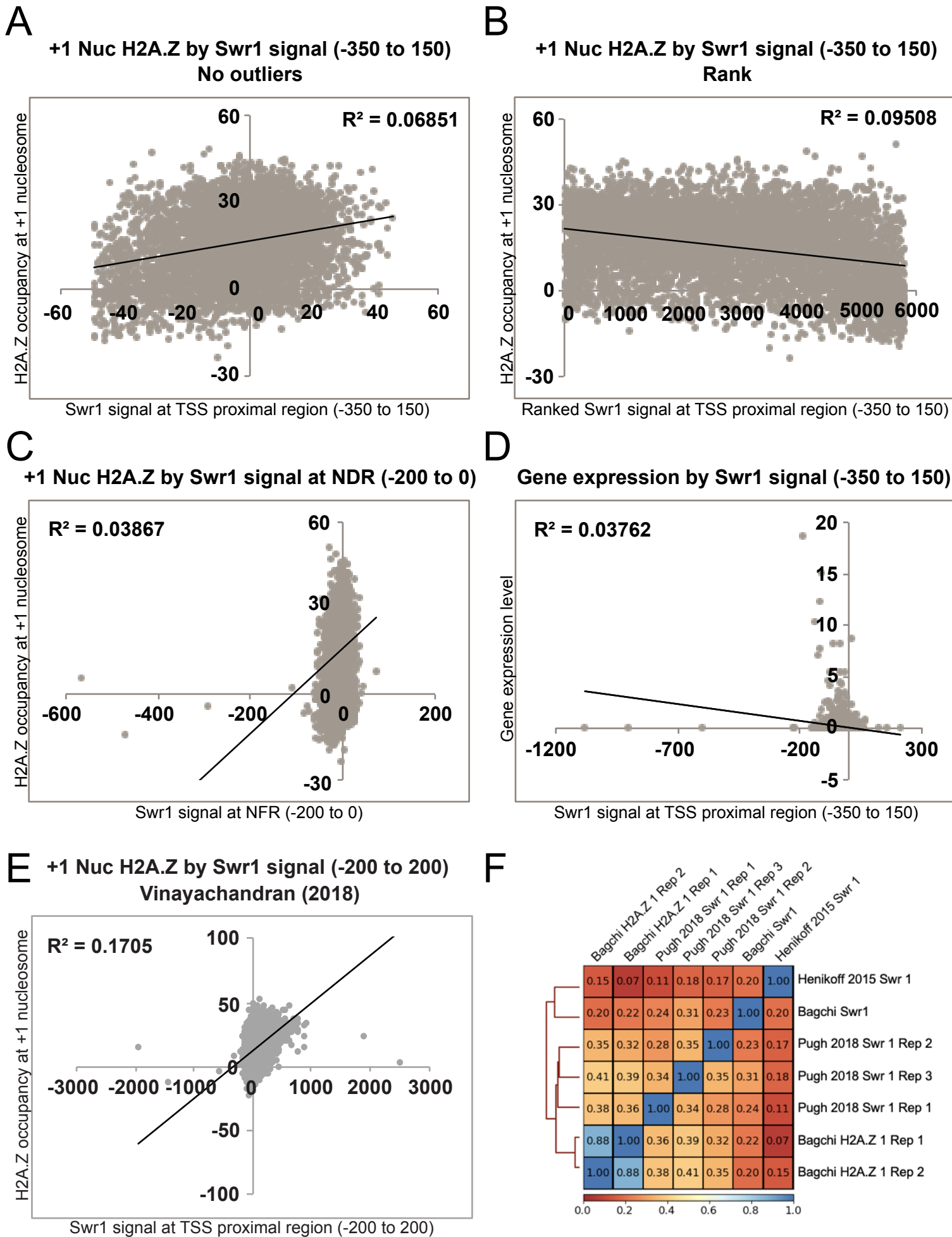
Supplementary Figure S4



Supplementary Figure S5



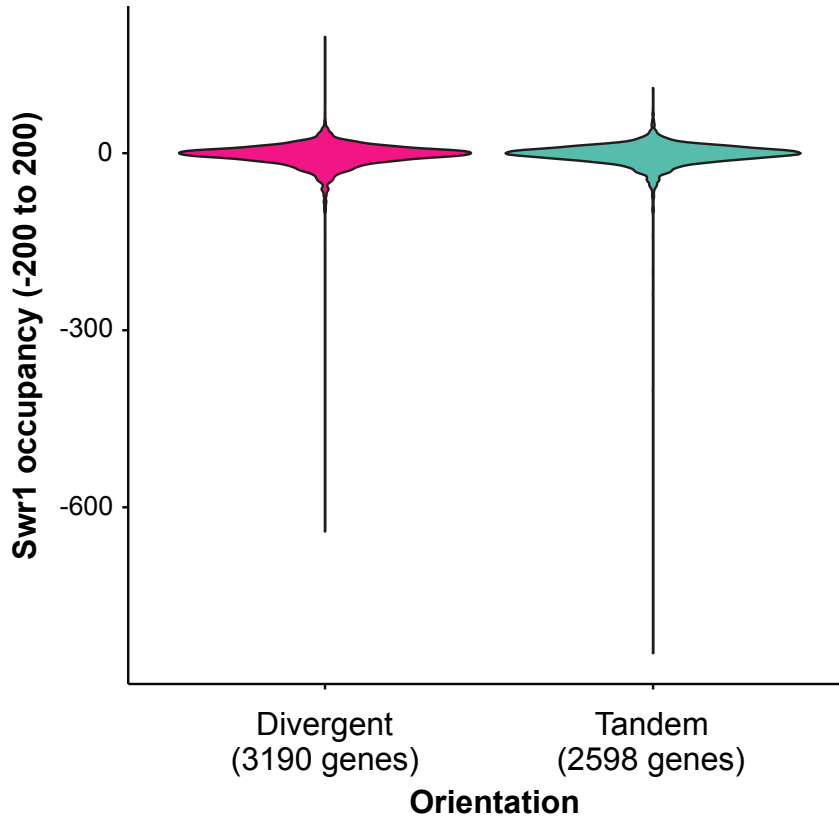
Supplementary Figure S6



Supplementary Figure S7

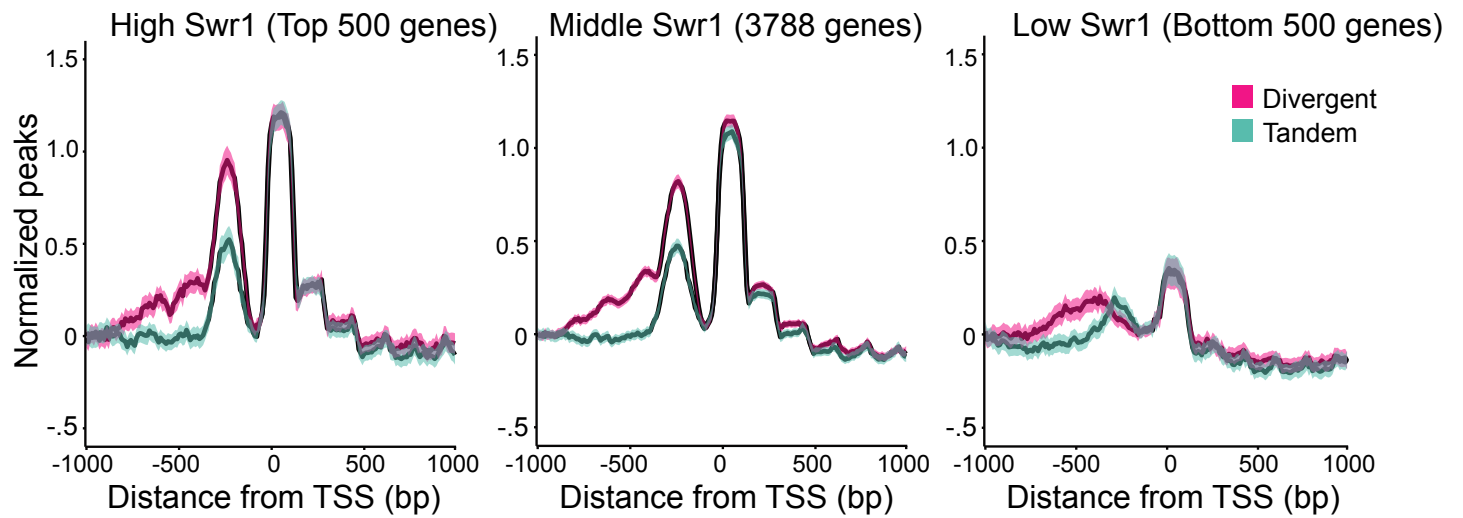
A

Swr1 occupancy

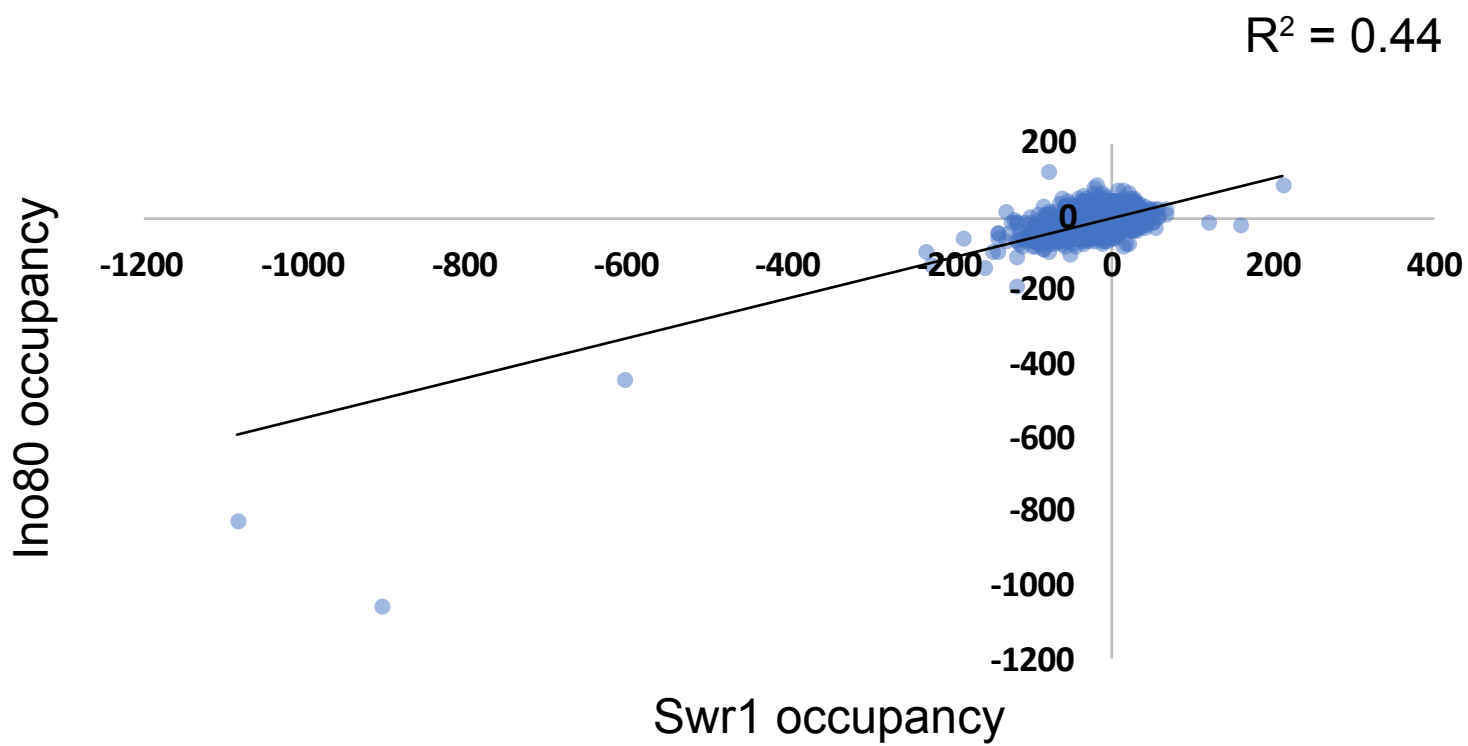


B

H2A.Z incorporation

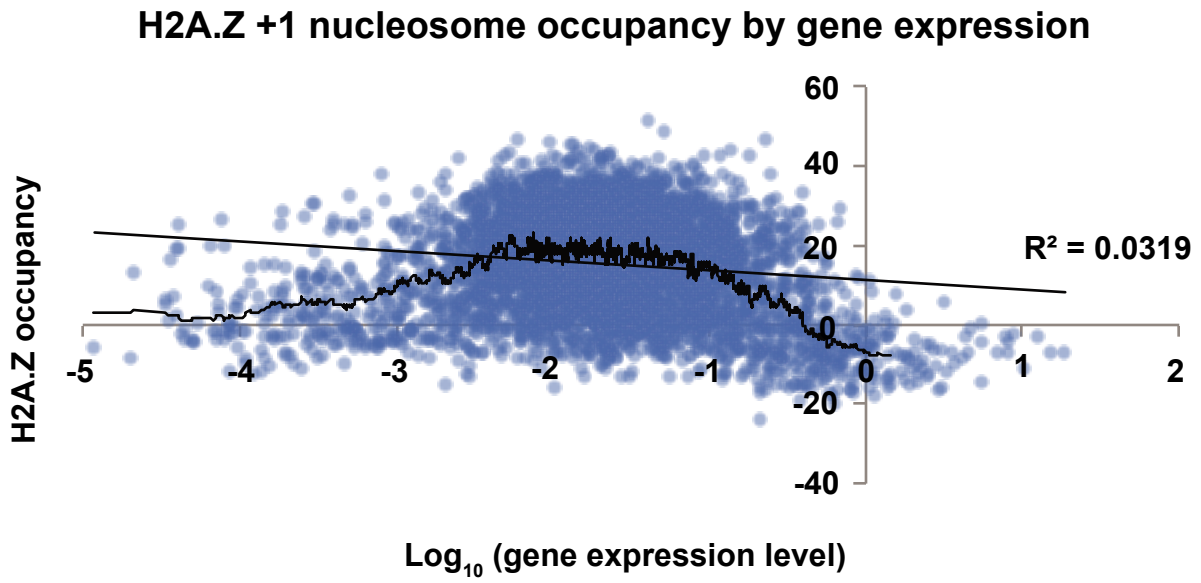


Supplementary Figure S8

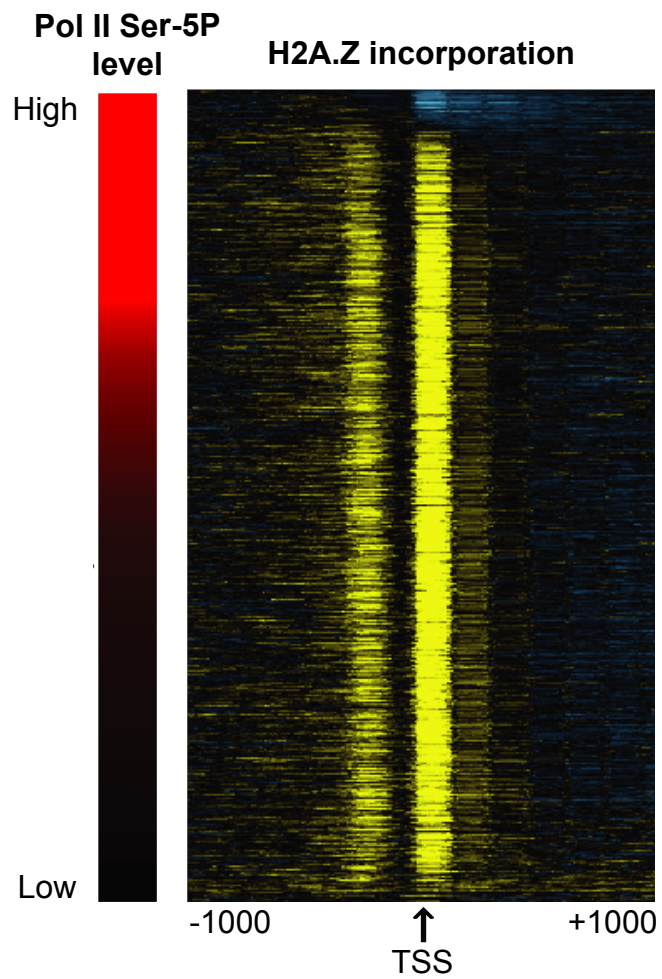


Supplementary Figure S9

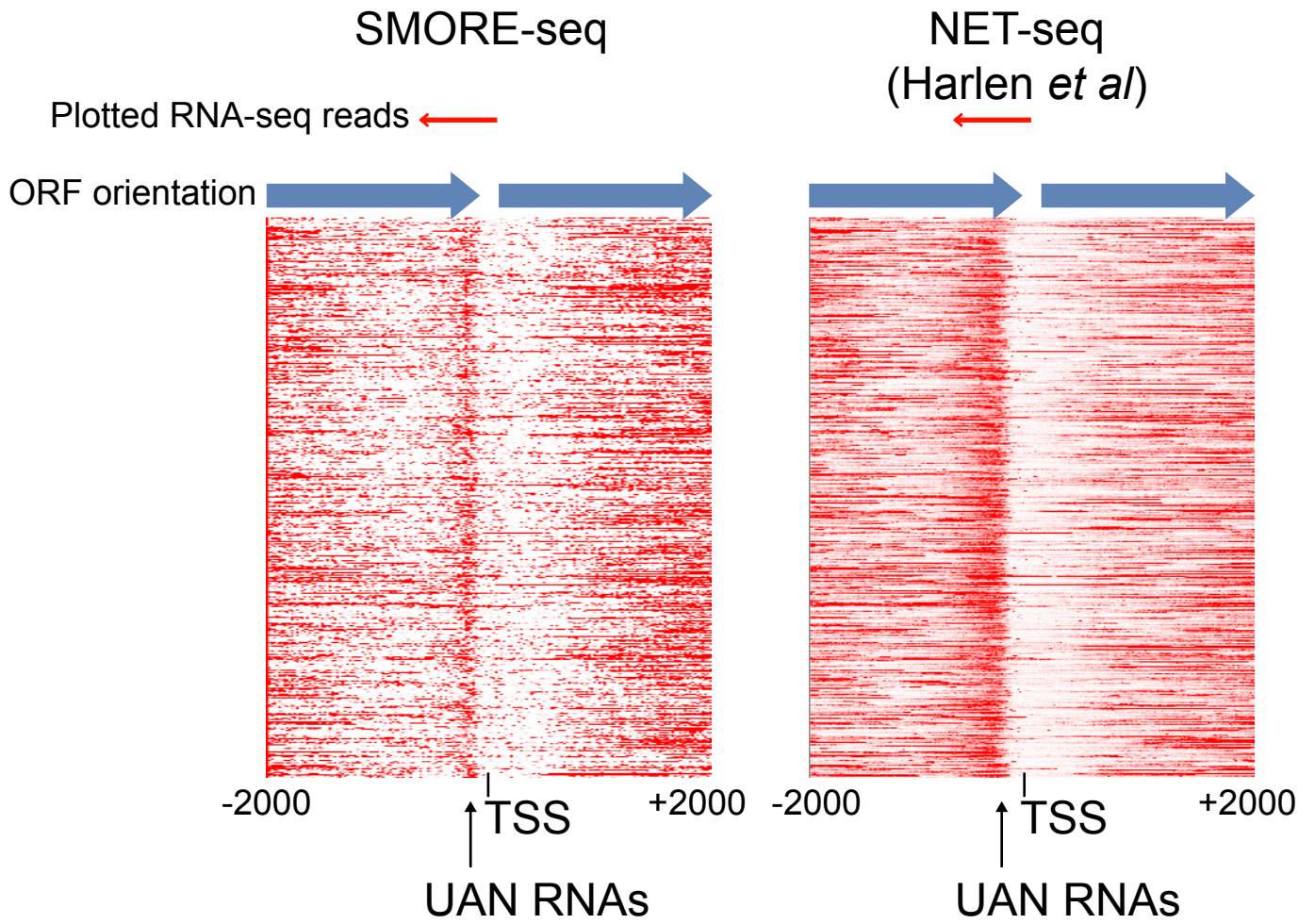
A




B

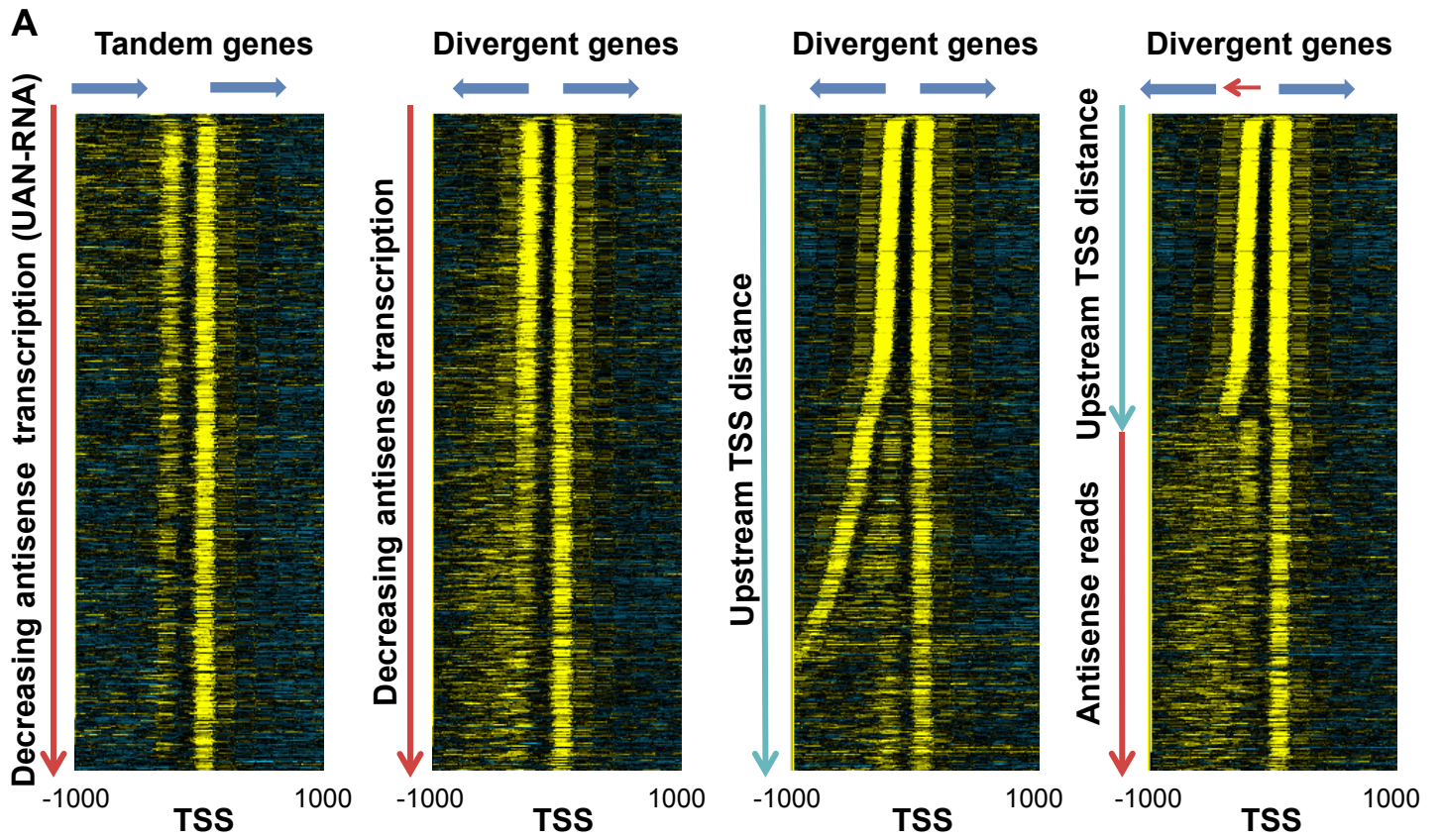


Supplementary Figure S10



Supplementary Figure S11

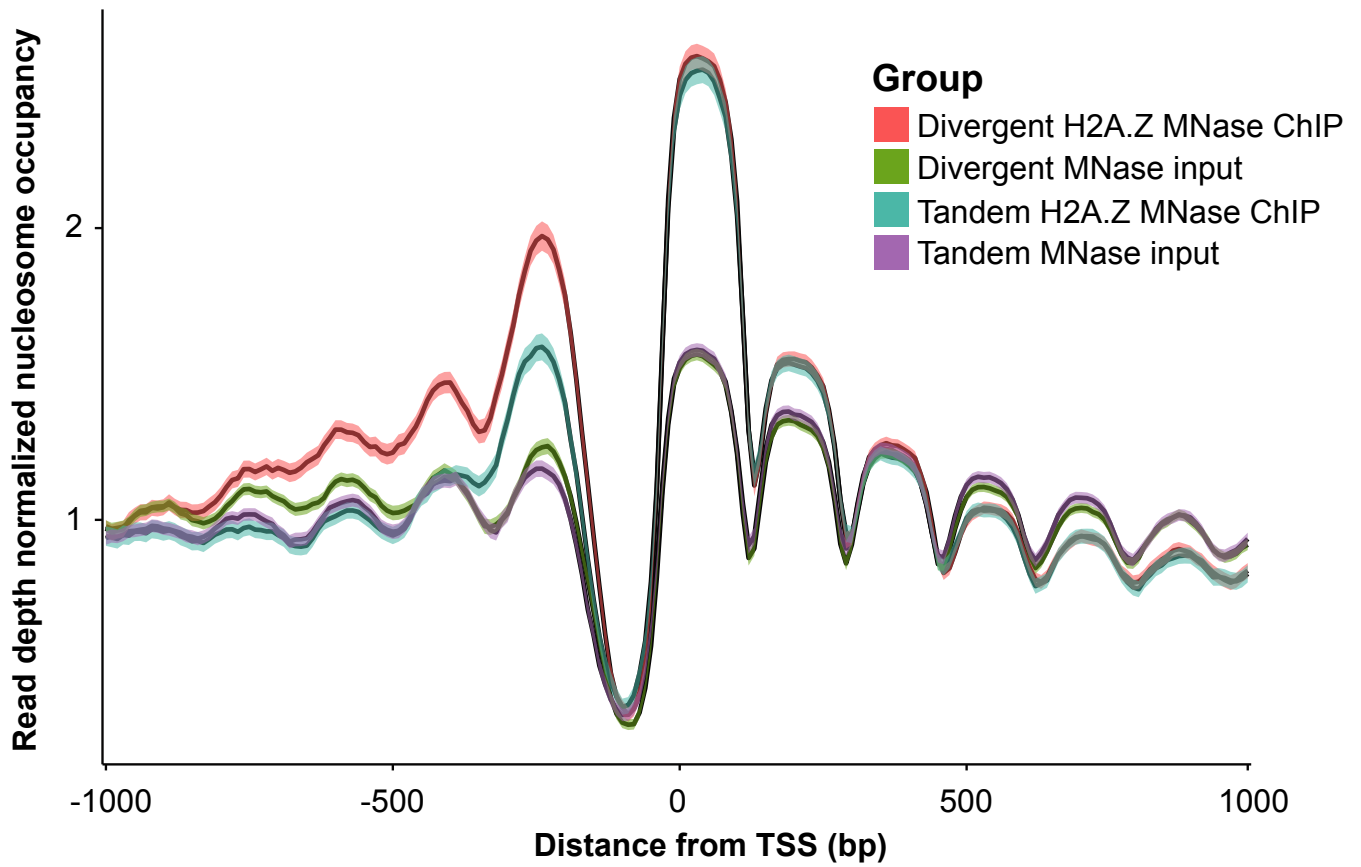
Legend  ORF
 UAN-RNA



Supplementary Figure S12

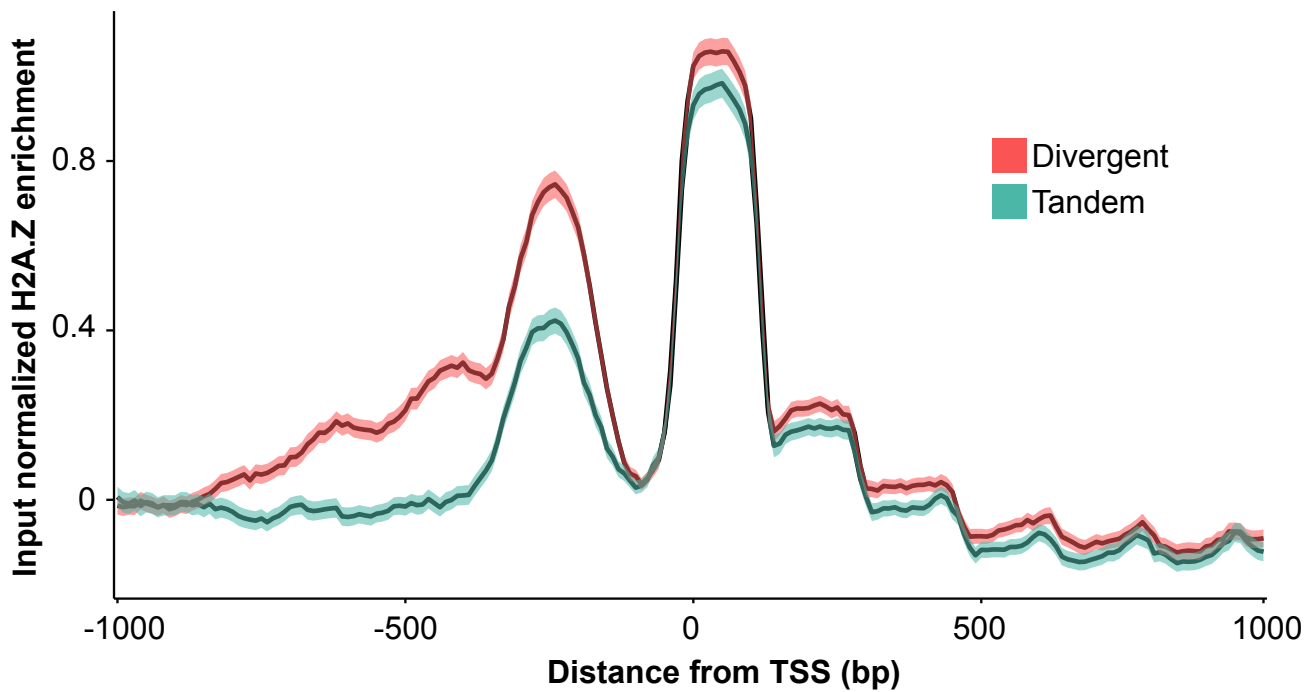
A

Average read enrichment profiles

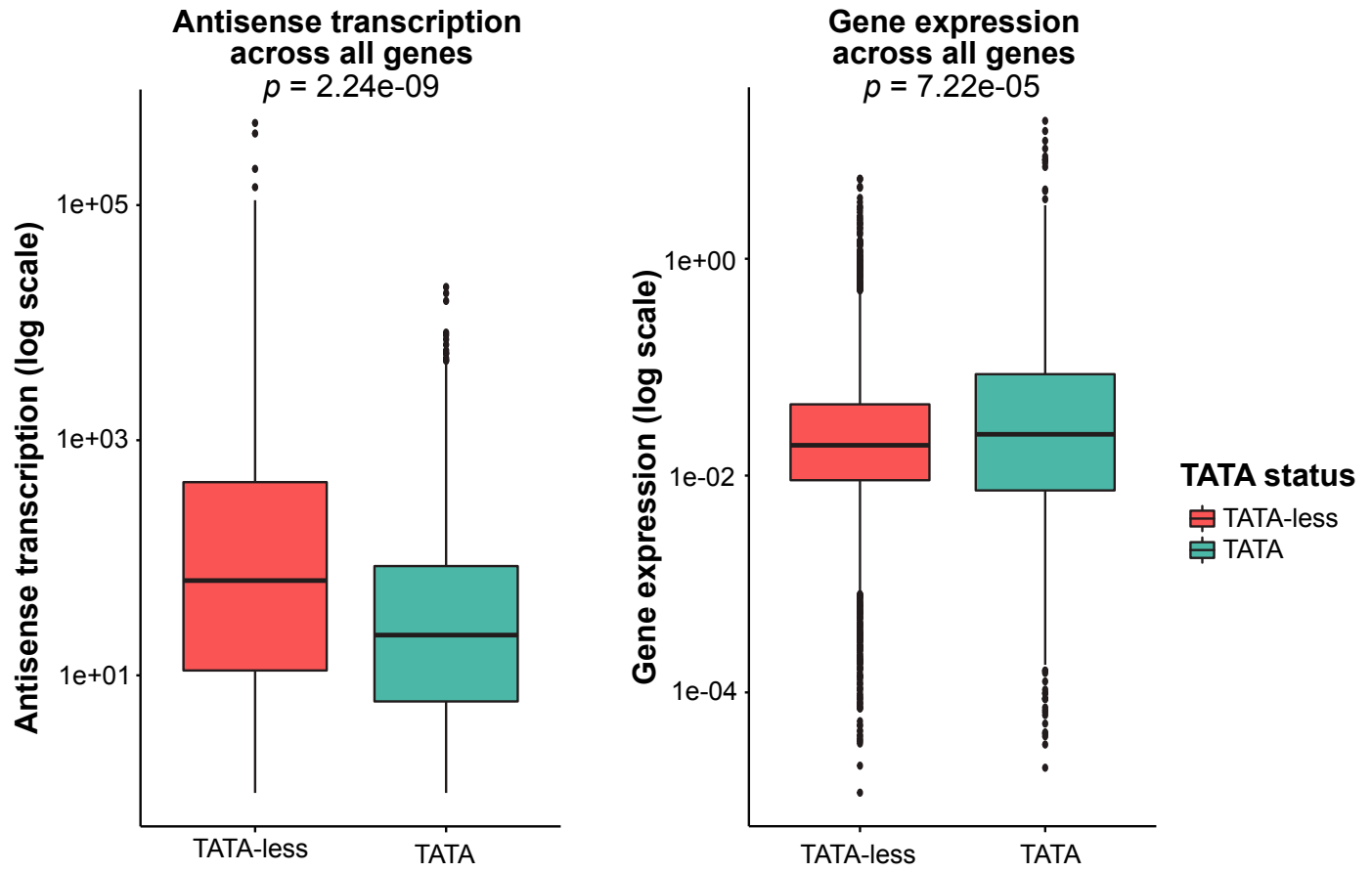


B

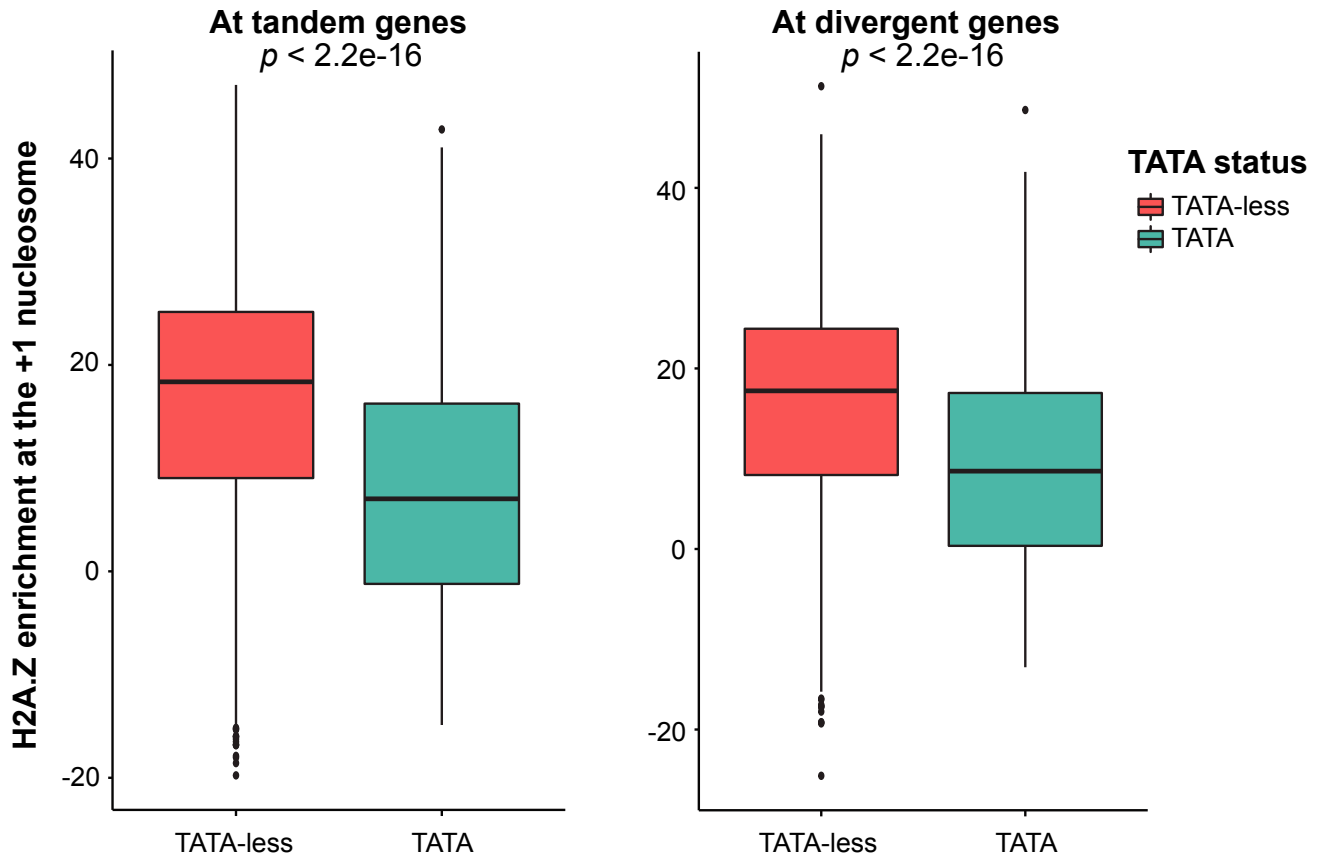
Average input-normalized H2A.Z occupancy profiles



Supplementary Figure S13

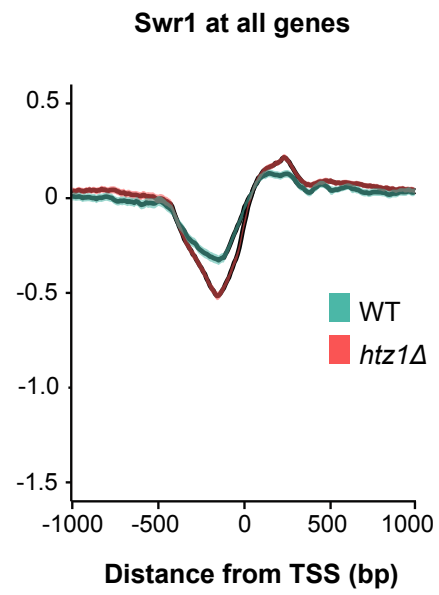
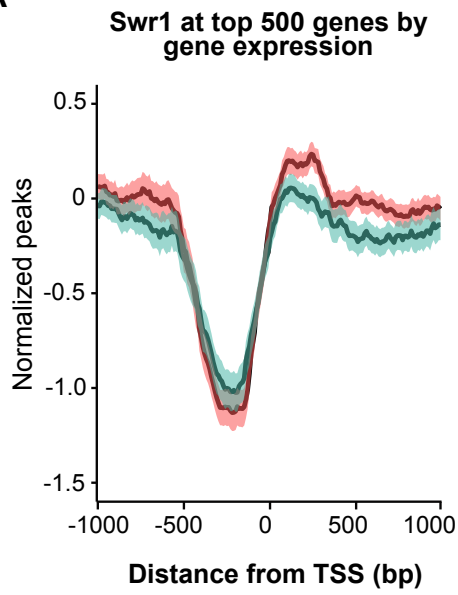


Supplementary Figure S14

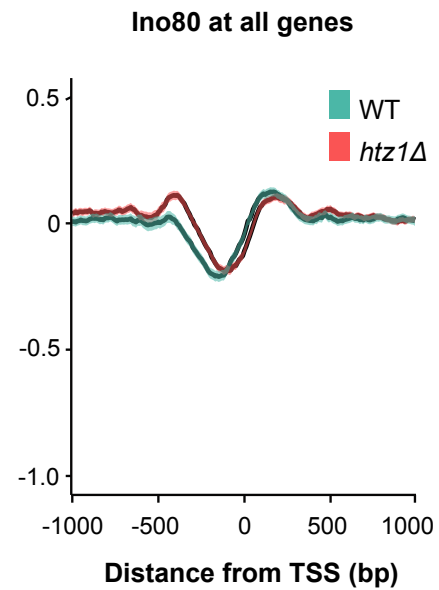
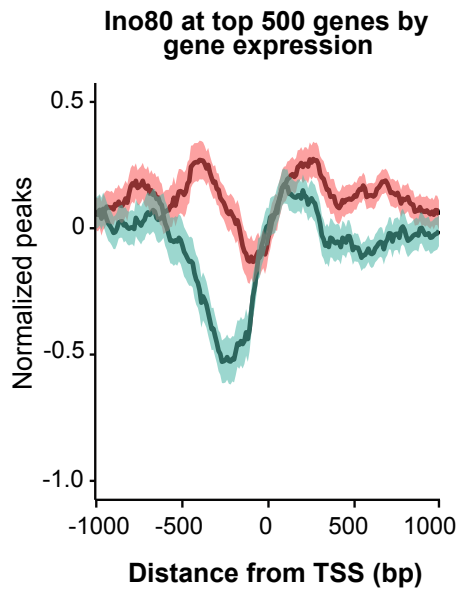


Supplementary Figure S15

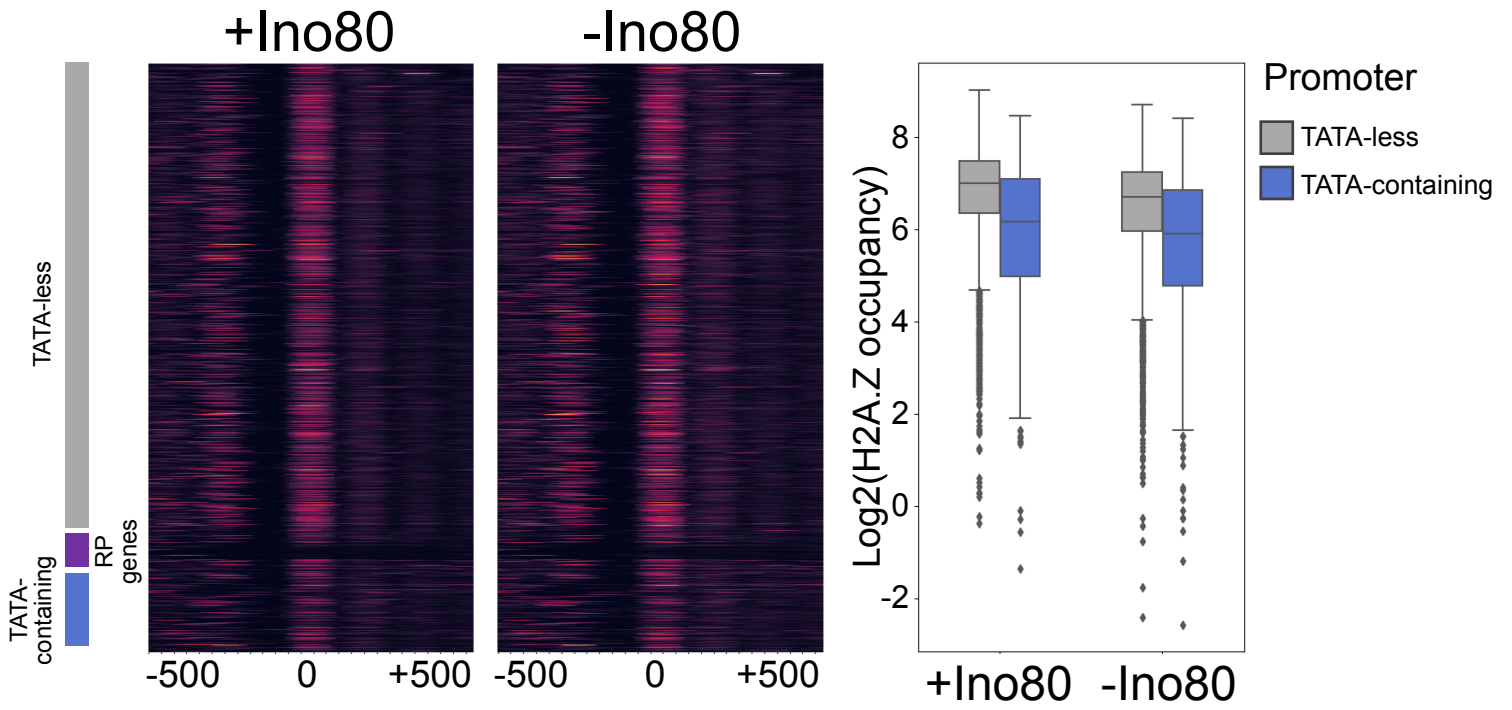
A



B



Supplementary Figure S16



Supplementary Figure S17

